Synthesis of a natural core substrate with lignin-xylan cross-linkage for unveiling the productive kinetic parameters of glucuronoyl esterase

Koh, Sangho ; Saito, Yasuko ; Kudo, Hisashi ; Taguchi, Seiichi ; Kumagai, Akio ; Mizuno, Masahiro ; Samejima, Masahiro ; Amano,…

(URL)
https://hdl.handle.net/20.500.14094/0100491634

Synthesis of a natural core substrate with lignin-xylan cross-linkage for unveiling the productive kinetic parameters of glucuronoyl esterase

Sangho Koh [a,*,1], Yasuko Saito [b], Hisashi Kudo [c], Seiichi Taguchi [c,d], Akio Kumagai [b], Masahiro Mizuno [e], Masahiro Samejima [e], Yoshihiko Amano [e,**]

[a] Department of Bioscience and Textile Technology, Interdisciplinary Graduate School of Science and Technology, Shinshu University, 4-17-1 Wakasato, Nagano, 380-8553, Japan
[b] Research Institute for Sustainable Chemistry, Department of Materials and Chemistry, National Institute of Advanced Industrial Science and Technology (AIST), 3-11-32 Kagamiyama, Higashi-Hiroshima, Hiroshima, 737-0046, Japan
[c] Graduate School of Science, Technology and Innovation, Kobe University, 1-1 Rokkodai-cho, Nada-ku, Kobe, Hyogo, 657-8501, Japan
[d] Department of Chemical Science and Engineering, Graduate School of Engineering, Kobe University, 1-1 Rokkodaicho, Nada-ku, Kobe, Hyogo, 657-8501, Japan
[e] Faculty of Engineering, Shinshu University, 4-17-1 Wakasato, Nagano, 380-8553, Japan

ARTICLE INFO

ABSTRACT

Lignin-carbohydrate complexes (LCCs) present a considerable hurdle to the economic utilization of lignocellulosic biomass. Glucuronoyl esterase (GE) is an LCC-degrading enzyme that catalyzes the cleavage of the cross-linkages between lignin and xylan in LCCs. Benzyl-D-glucuronate (Bn-GlcA), a commercially available substrate, is widely used to evaluate GE activity assays. However, since Bn-GlcA lacks the structural backbone of naturally occurring LCCs, the mechanisms underlying the activity of GEs and their diversity in the structure-activity relationship are not fully understood. Herein, we provided a synthesis scheme for designing $1,2^3$-α-D-(6-benzyl-4-O-methyl-glucuronyl)-1,4-β-D-xylotriose (Bn-MeGlcA^{3}Xyl$_3$) as a natural core substrate bearing cross-linkage between lignin and glucuronoxylan. A well-defined and yet more realistic synthetic substrate was successfully synthesized via a key step of the benzyl esterification of 4-O-methyl-glucuronyl-1,4-β-D-xylotriose (MeGlcA^{3}Xyl$_3$), a minimized fragment of glucuronoxylan enzymatically digested by β-1,4-xylanase. To the best of our knowledge, this is the first report of the productive GE kinetic analysis using this substrate. Kinetic parameters of the GE from the fungal *Pestalotiopsis* sp. AN-7 (*Pes*GE), i.e., the K_m, V_{max}, and k_{cat} of Bn-MeGlcA^{3}Xyl$_3$, were 0.43 mM, 55.5 µmol min^{-1}·mg^{-1}, and 35.8 s^{-1}, respectively. On the other hand, as reported to date, the productive kinetic parameters for Bn-GlcA were not obtained because of its excessively high K_m value (>16 mM). The substantial variance in the enzymatic activity of *Pes*GE regarding substrate-binding affinity between Bn-MeGlcA^{3}Xyl$_3$ and Bn-GlcA was also demonstrated using *in silico* docking simulation. These results suggested that the extended xylan fragment is a key structural determinant affecting *Pes*GE's substrate recognition. Furthermore, the presence of a natural xylan backbone allows for evaluating the enzyme activity of xylan-degrading enzymes. Accordingly, the synthesized substrate with the natural core structure of LCC allowed us to unveil the productive kinetic parameters of GEs, serving as a versatile substrate for further elucidating the cascade reaction of GE and xylan-degrading enzymes.

1. Introduction

Lignocellulosic biomass is the most abundant renewable carbon source on Earth [1]. Facilitating the economic conversion of lignocellulose to yield value-added biochemicals, biofuels, and bioplastics is a central objective for fostering a sustainable circular bioeconomy. However, the lignocellulose structure is highly complex and resistant to enzymatic and chemical degradation because of a heteropolymeric complex composed of lignin and hemicellulose, i.e., lignin-carbohydrate complexes (LCCs). LCCs confer rigidity to lignocellulose by bridging the lignin and hemicellulose biopolymers, improving their physical and chemical properties. Therefore, effectively separating lignin and hemicellulose in LCCs is crucial for deconstructing lignocellulose in industrial biomass refinery processes.

Ester bonds between lignin and glucuronoxylan are the major chemical cross-linkages in the LCCs of lignocellulosic woody biomass. The carboxyl group of 4-*O*-methyl glucuronic acid (MeGlcA) in the xylan main chain and the lignin hydroxyl group represent an important ester linkage in birchwood (*Betula*) species [2]. Glucuronoyl esterase (GE) is an LCC-degrading enzyme that catalyzes the cleavage of ester linkages between lignin phenolic groups and xylan MeGlcA carboxyl side chain groups [3]. GE may have potential in the paper industry for chemical pulp production as part of an enzymatic bleaching process. GE enzymatic properties were first determined using an enzyme purified from the culture fluid of *Schizophyllum commune* [4]. The *cip2* gene was

identified from *Trichoderma reesei* based on its partial amino acid sequence [5], leading to the discovery of a new carbohydrate esterase family, namely, carbohydrate esterase family 15, in the carbohydrate-active enzymes database (http://www.cazy.org/). A substrate containing an ester bond between lignin and xylan, similar to those found in LCCs, is required to evaluate GE activity. Although LCC extraction from plant cell walls has been previously reported [6], producing well-defined LCCs remains challenging. Furthermore, the complex structure–property relationship of LCCs impedes the preparation of well-defined yet soluble substrates. These challenges lead to numerous unanswered questions regarding the underlying catalytic mechanisms of GEs and their physiological role in cell wall degradation in natural environments.

Generally, molecular mechanisms underlying the activity of the target enzyme should be understood in-depth as a complexed form with the natural substrate. However, due to several limitations, including the challenging synthesis of natural substrates, we should frequently consider enzymatic information obtained using commercially available easy-to-use substrates as tentative data. Especially, polymeric complexed substrates, such as LCCs, are typical. This issue does not allow us to evaluate the productive enzymatic activity, leading to a gap in knowledge. Therefore, synthesizing natural substrates of interest will serve as a crucial milestone, opening new avenues to explore the essential sites that directly interact with the active sites of counter enzymes.
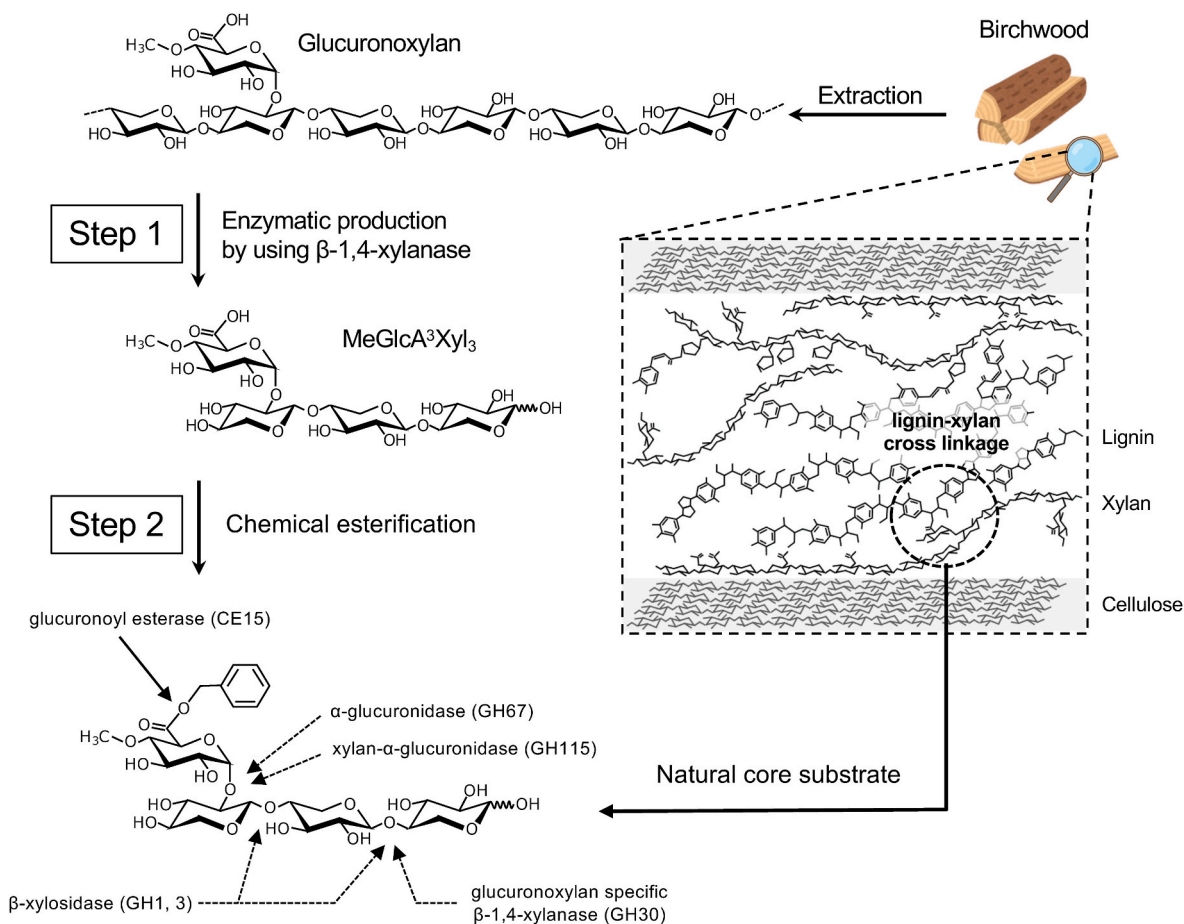
Fig. 1. Scheme for the chemo-enzymatic synthesis of a natural core structure bearing a benzyl ester cross-linkage between lignin and xylan in lignin-carbohydrate complexes (LCCs). Step 1: enzymatic production of MeGlcA³Xyl₃ through enzymatic digestion by β-1,4-xylanase from birchwood glucuronoxylan, as described in our previous study [7]. Step 2: chemical synthesis of Bn-MeGlcA³Xyl₃ through benzyl esterification. Bn-MeGlcA³Xyl₃ bears a natural core structure of LCCs that possesses multiple cleavage sites potentially degradable by carbohydrate esterase (CE) family 15: GEs [3], glycosyl hydrolase (GH) family 30: xylanases [8], GH family 1 and 3: β-xylosidases, and GH family 67 and 115: α-glucuronidases [9].

In the present study, we aimed to shed light on this challenge. In the case of LCCs, commercially accessible benzyl glucuronate (Bn-GlcA) has been utilized as a conventional substrate for evaluating the enzymatic activity of GE. Recently, the substrate binding of fungal *Cu*GE with a MeGlcA-branched xylotrisaccharide, 1,2³-α-D-(4-*O*-methyl-glucuronyl)-1,4-β-D-xylotriose (MeGlcA³Xyl₃) was elucidated, indicating that the xylotriose segment is important for substrate recognition by GE. However, Bn-GlcA lacks the structural backbone of LCCs, i.e., the naturally occurring 4-*O*-methyl group of MeGlcA and the xylan segment. Here, we aimed to synthesize a new substrate bearing the natural core structure of LCC. To achieve this goal, we designed a bottom-up synthetic strategy for synthesizing a target structure containing a benzyl ester moiety and MeGlcA-branched xylotrisaccharide, 1,2³-α-D-(4-*O*-methyl-glucuronyl)-1,4-β-D-xylotriose (MeGlcA³Xyl₃) (Fig. 1). First, MeGlcA³Xyl₃ was enzymatically produced by completely degrading MeGlcA-branched glucuronoxylan using the endo-β-1,4-xylanase *Pes*Xyn10A from *Pestalotiopsis* sp. AN-7 based on our previous study [7]. Second, Bn-MeGlcA³Xyl₃ was chemically synthesized by benzyl esterification of the MeGlcA C6 carboxyl group. Herein, the newly synthesized substrate Bn-MeGlcA³Xyl₃ was justified for a natural core substrate through kinetic analysis and the *in silico* docking simulation of the fungal GE from *Pestalotiopsis* sp. AN-7 (*Pes*GE). Furthermore, this bottom-up synthesis approach enables the acquisition of the naturally occurring xylan segment, which can be degraded by xylan-degrading enzymes, such as xylanases [8], β-xylosidases [8], and MeGlcA-debranching enzyme α-glucuronidases [9]. This versatility provides the molecular basis for investigating synergistic breakdown mechanisms involving GEs and other xylan-degrading enzymes and accelerates the development of powerful engineered and/or evolved enzymes for industrial biomass refineries.

2. Materials and methods

2.1. Chemicals and enzymes

Benzyl D-glucuronic acid (Bn-GlcA) was purchased from Carbosynth (Compton, UK) and used as a substrate for determining the optimal pH, temperature, and stability. Birchwood xylan, a glucuronoxylan, was purchased from Sigma-Aldrich (St. Louis, MO, USA) and used as the starting material for the chemical synthesis of Bn-MeGlcA³Xyl₃. All other chemicals were of analytical grade. The in-house-prepared endo β-1,4-xylanase *Pes*Xyn10A (GenBank accession No. BCL51556.1) was produced recombinantly using the *Pichia pastoris* expression system and subsequently purified as described in our previous study [7].

2.2. Synthesis and purification of Bn-MeGlcA³Xyl₃

To prepare MeGlcA³Xyl₃, 10 g of birchwood glucuronoxylan was treated with 254 U of *Pes*Xyn10A and then enzymatically digested at 40 °C. The resulting hydrolysate was subjected to tandem column gel permeation chromatography (GPC) using HiLoad 26/60 Superdex 30 PG (ID. 260 × 600 mm; GE Healthcare Life Sciences, Uppsala, Sweden) on an XK16/40 Sephadex G-10 column (ID. 16 mm × 400 mm; GE Healthcare Life Sciences) using a BioLogic DuoFlow system (Bio-Rad Laboratories, Hercules, CA, USA). The mobile phase consisted of deionized water with a flow rate of 3.0 mL min⁻¹. The eluted fraction was monitored using a high-performance liquid chromatography (HPLC) system connected to a SUGAR KS-802 column (Resonac, Tokyo, Japan) with a refractive index detector. Purified MeGlcA³Xyl₃ (0.51 g, 0.84 mmol) was dissolved in dry *N,N*-dimethylformamide (20 mL) and cooled on ice. Tetra-*n*-butylammonium fluoride (0.92 mL, 0.92 mmol, 1.1 equiv.; 1 M tetra-*n*-butylammonium fluoride solution in tetrahydrofuran) and benzyl bromide (0.147 mL, 1.24 mmol) were added to the solution, and the reaction mixture was stirred at 25 °C for 20 h under N₂ gas (1 atm). After 20 h, the solvent was evaporated using toluene (400 mL). The residue was purified using silica gel column chromatography

(chloroform/methanol/H₂O, 70/30/5, v/v/v) to obtain Bn-MeGlcA³Xyl₃ as a colorless oil (0.26 g, 0.38 mmol, 45 mol% yield). The reaction mixture was evaluated using thin-layer chromatography (TLC) on silica gel 60 F₂₅₄ plates (Merck, Darmstadt, Germany) with a chloroform/methanol/H₂O (70/30/5, v/v/v) mobile phase. After spraying with methanol containing 3 % sulfuric acid, the spots were visualized under ultraviolet (UV) light, followed by heating to 100 °C for 5 min. Purified MeGlcA³Xyl₃ and Bn-MeGlcA³Xyl₃ were dissolved in deuterated dimethyl sulfoxide (DMSO-d6) and characterized by nuclear magnetic resonance (NMR) spectroscopy using a 400-MHz DD2 NMR spectrometer equipped with a ONE probe (Agilent Technologies, Santa Clara, CA, USA), with control and processing conducted using VnmrJ4.2 software (Agilent Technologies). ¹H, ¹³C, ¹H–¹H correlation spectroscopy (COSY), ¹³C–¹H heteronuclear single quantum coherence (HSQC), ¹³C–¹H heteronuclear multiple bond connectivity (HMBC), and HSQC-totally correlated spectroscopy (HSQC-TOXSY) NMR spectra were acquired using the Agilent standard pulse sequences "Proton," "Carbon," "Gradient COSY," "Gradient HSQCAD," "Gradient HMBCAD," and "Gradient HSQC-TOXY," respectively. Central DMSO peaks were used as internal references (δ¹³C/δ¹H: 39.5/2.49 ppm).

2.3. Production and purification of recombinant PesGE

The cDNA sequence of the mature region of *Pes*GE (GenBank accession No. BCL51557.1) was inserted into the pPIC9K vector under the α-factor signal sequence for secretory expression. The resulting recombinant expression vector was linearized with *Sal*I and introduced into *P. pastoris* GS115 using electroporation. The *P. pastoris* transformants were grown in flasks in a shaking incubator (200 rpm) at 30 °C for 4 days, with methanol addition every 24 h to maintain *Pes*GE induction. Thereafter, culture supernatants were analyzed to monitor *Pes*GE production using sodium dodecyl sulfate-polyacrylamide gel electrophoresis (SDS-PAGE) with a 10 % polyacrylamide gel. Subsequently, the secreted *Pes*GE was precipitated from the culture medium by adding ammonium sulfate at 90 % saturation, after which the precipitate was collected by centrifugation and dissolved in 50 mM sodium acetate buffer (pH 5.0) containing 30 % saturated ammonium sulfate. Next, the enzyme solution was subjected to TOYOPEARL Butyl-650 M column chromatography (ID. 2.5 mm × 230 mm; Tosoh Corporation, Tokyo, Japan) using a BioLogic DuoFlow 40F base system (Bio-Rad Laboratories). Non-adsorbed proteins were eluted with the same buffer and the adsorbed proteins were eluted by linearly decreasing the ammonium sulfate concentration. The eluted fractions were subjected to SDS-PAGE. Protein quantity was measured using a protein assay kit (Bio-Rad Laboratories) with bovine serum albumin as the standard.

2.4. Enzyme kinetics of PesGE

The pH and temperature responses of *Pes*GE were assessed by measuring the amounts of hydrolyzed benzyl alcohol from the reaction with 0.5 mM Bn-Glc. To determine the optimal pH for *Pes*GE activity, the enzymatic reaction was conducted at 30 °C for 10 min using potassium phosphate buffer (pH 2 to 3), sodium acetate buffer (pH 4 to 6), and Tris-hydrochloride acid buffer (pH 7 to 9). To determine pH stability, *Pes*GE was incubated with buffers adjusted to different pH values for 6 h at 30 °C, followed by reaction at pH 5.0 and 30 °C for 10 min. To determine the optimum temperature, the enzymatic reaction was conducted at temperatures ranging from 30 to 70 °C at a pH of 5.0 for 30 min. Thermal stability was assessed by incubating *Pes*GE at various temperatures (30–70 °C) at pH 5.0 for 6 h, followed by reaction at 30 °C and pH 5.0 for 10 min.
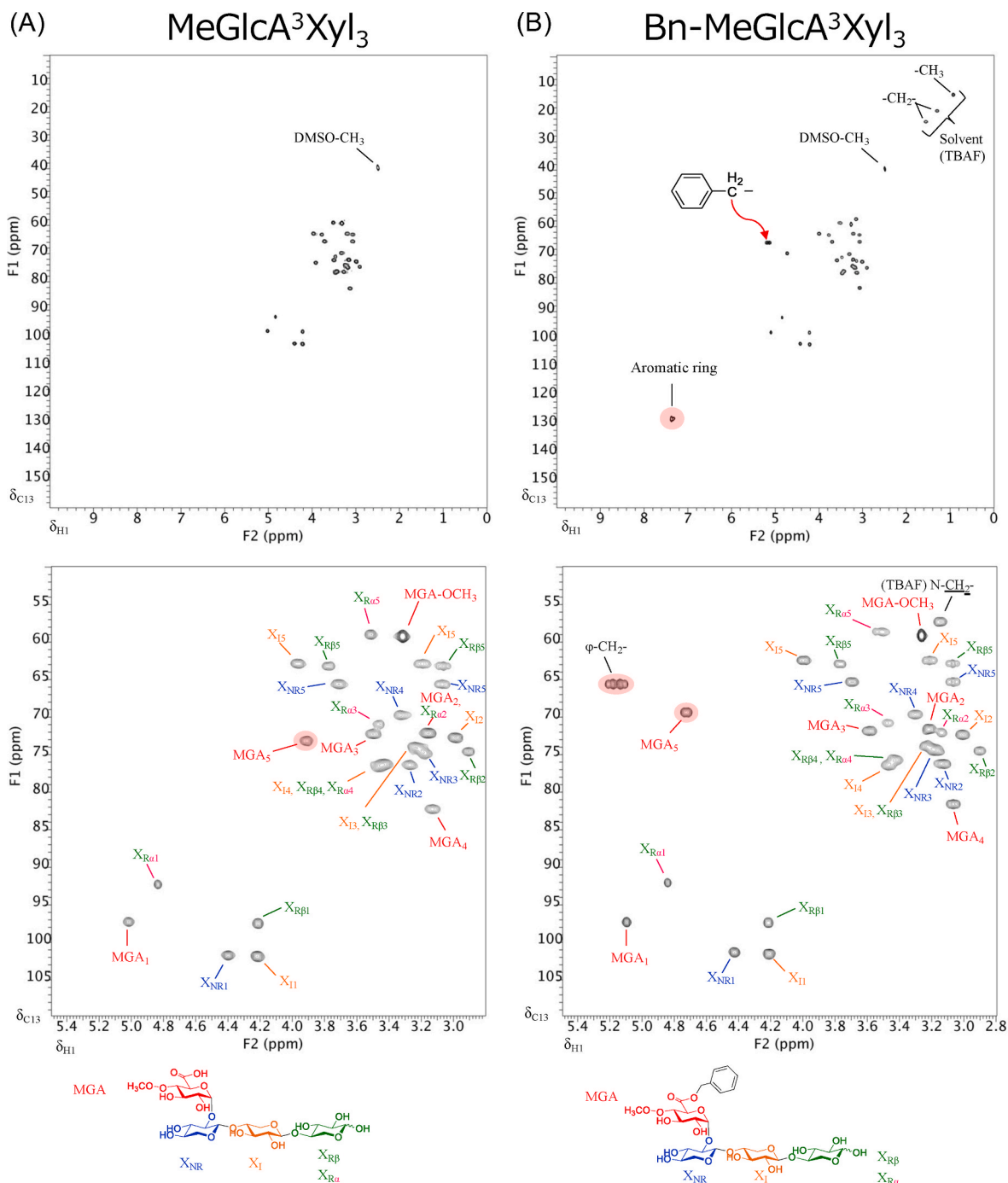
Kinetic parameters were determined using enzymatic hydrolysis at 30 °C for 20 min in 100 mM sodium acetate buffer (pH 5.0), Bn-GlcA [0.50–12.0 mM in 10 % DMSO, Bn-MeGlcA³Xyl₃ (0.06–3.74 mM in 10 % DMSO), *Pes*GE (0.5–5.0 µg mg⁻¹)]. At each time point, 100 µL of glacial acetic acid was added to halt the reaction. Benzyl alcohol release

was monitored using an HPLC system connected to an Inertsil ODS-3 column (5.0 μm, ID. 4.6 mm × 150 mm; GL Sciences Inc., Tokyo, Japan) at a wavelength of 245 nm, with a UV detector. Non-linear curve fitting to the Michaelis–Menten equation was used to determine K_m and V_{max} values.

2.5. In silico docking analysis

The *Pes*GE structure model was generated using AlphaFold2 [10]. Molecular docking analysis with Bn-MeGlcA^{3}Xyl$_3$ and Bn-GlcA was performed using Molecular Operating Environment (MOE) software

(version 2019.01; Chemical Computing Group, Montreal, QC, Canada). Initially, the *Cu*GE crystal structure (PDB ID: 6RV8 [11]) was superimposed on the *Pes*GE model, after which all crystal structures, except that for MeGlcA^{3}Xyl$_3$ from 6RV8, were eliminated. The ligand molecule MeGlcA^{3}Xyl$_3$ was then replaced with Bn-MeGlcA^{3}Xyl$_3$, Bn-GlcA^{3}Xyl$_3$, Bn-MeGlcA, and Bn-GlcA using the MOE builder. The model was then protonated at a pH of 7 and temperature of 300 K using the protonate 3D tool of MOE, followed by optimization through energy minimization using the AMBER10:extended Hückel theory (EHT) force field (gradient = 0.01 RMS kcal mol^{-1} A^{-2}). For docking simulation, the AMBER10: EHT force field and the implicit solvation model of the reaction field

Fig. 2. 2D HSQC-NMR structural confirmation of Bn-MeGlcA^{3}Xyl$_3$ (A) before and (B) after benzyl esterification reaction. The cross peaks assigned to the benzyl ester (marked in red) are clearly present in (B) after the benzyl esterification reaction, indicating that Bn-MeGlcA^{3}Xyl$_3$ was successfully synthesized. The signals of (A) MeGlcA^{3}Xyl$_3$ and (B) Bn-MeGlcA^{3}Xyl$_3$ are assigned in Tables S1 and S2, respectively. R: reducing end, I: internal unit, NR: non-reducing end, X: xylose unit, MGA: MeGlcA.

(R-field 1:80; cutoff 8, 10) were selected. The binding affinities of *Pes*GE toward the substrates were calculated using the GBVI/WSA dG scoring function with the Generalized Born solvation model (GBVI) [12,13]. This function is generally used to evaluate the free energy of the ligand docking simulation.

3. Results

3.1. Synthesis of Bn-MeGlcA³Xyl₃ as a natural core of LCC

To synthesize a natural core substrate containing naturally occurring LCCs, MeGlcA^{3}Xyl$_3$ was selected as the carbohydrate backbone for benzyl esterification. Based on our previous research [7], MeGlcA^{3}Xyl$_3$ was generated by digesting birchwood xylan using *Pes*Xyn10A, resulting in a final product that followed the hydrolysis pattern of GH10 endo β-1, 4-xylanase. Post-enzymatic reaction, MeGlcA^{3}Xyl$_3$ was isolated using GPC, yielding 1.6 g/10 g of xylan (dry mass; Fig. S1). LC-MS and HSQC-NMR analyses were conducted on the product, and the corresponding molecular ion peaks and chemical shifts of the isolated material were attributed to MeGlcA^{3}Xyl$_3$ (Fig. 2A).

Next, MeGlcA^{3}Xyl$_3$ was esterified with benzyl bromide (Bn-Br) and tetra-*n*-butylammonium fluoride to yield Bn-MeGlcA^{3}Xyl$_3$. The reaction product was purified using silica gel chromatography (Fig. S2), and its chemical structure was confirmed based on the HSQC-NMR spectra (Fig. 2B). After benzylation, the signals at δ_{1H} 7.33, 7.37 ppm; δ_{13C} 135.87, 128.41, 128.03, 127.87 ppm corresponding to the aromatic ring and δ_{1H} 5.08–5.22 ppm; δ_{13C} 65.81 ppm corresponding to the methylene group were observed. Additionally, the signal assigned to the C5/H5 of the MeGlcA unit shifted from δ_{13C}/δ_{1H} = 73.37/3.91 ppm to δ_{13C}/δ_{1H} = 69.57/4.71 ppm after benzylation, indicating esterification between the carboxylic acid of the MeGlcA unit and benzyl bromide. These results support the successful synthesis of the target compound Bn-MeGlcA^{3}Xyl$_3$ at a yield of 45 % from MeGlcA^{3}Xyl$_3$.

3.2. Cloning and heterologous expression of PesGE in P. pastoris

Here, degradability of Bn-MeGlcA^{3}Xyl$_3$ was evaluated using recombinant *Pes*GE previously cloned from *Pestalotiopsis* sp. AN-7 [7] and newly expressed in *P. pastoris*. Based on BLAST analysis, the deduced amino acid sequence of *Pes*GE showed high homology with those of characterized GEs: *Nc*GE from *Neurospora crassa* (65 %, NCU09445) [14], *Lf*GE2 from *Lentithecium fluviatile* (60 %, jgi311197) [15], *St*GE2 from *Myceliophthora thermophila* (63 %, PDB ID: 4G4G, AEO60464.1) [16], *Pa*GE1 from *Podospora anserina* S mat⁺ (54 %, CAP60908.1) [17], *Aa*GE1 from *Acremonium alcalophilum* (53 %, AOT21131) [18],

Trichoderma reesei (52 %, Cip2, PDB ID: 3PIC, AAP57749.1) [19], *Cu*GE from *Cerrena unicolor* (48 %, AIY68500.0) [11,20], and *Sc*GE from *Schizophyllum commune* H4-8 (48 %, XP_003026289.1) [21]. Based on the amino acid sequence alignment of the GEs, the conserved sequence VTGCGCSRXGKGA (Val207–Ala219), containing a nucleophilic serine residue (Ser213), was conserved in *Pes*GE (Fig. S3). Two additional consensus sequences constituting the catalytic triad for GEs, PQESG, and HC, containing glutamic acid (Glu236) and histidine (His346) residues, were also conserved in the *Pes*GE sequence. In contrast to Cip2, *Pes*GE lacks a carbohydrate-binding domain.

To characterize *Pes*GE, recombinant *Pes*GE was produced using the secretory expression system of *P. pastoris*. After purification using sequential column chromatography, recombinant *Pes*GE was detected as a single smeared band at approximately 45 kDa using SDS-PAGE, which was higher than the calculated molecular weight of the primary structure (39 kDa) (Fig. 3A). Thus, deglycosylation using endo-*N*-acetyl-D-glucosaminidase (PNGase F) resulted in a molecular weight decrease of approximately 39 kDa, suggesting that *Pes*GE is expressed as a glycosylated protein, with a potential *N*-glycosylation site at Asn27. Optimal *Pes*GE activity against Bn-GlcA was noted at pH 5, with the enzyme retaining over 90 % of its activity even after 24 h of incubation at 50 °C in a pH range of 4–8 (Fig. 3B). Analysis of the primary sequence and general properties indicate that *Pes*GE conforms to the characteristics of a typical fungal GE.

3.3. In vitro kinetic analysis of PesGE toward Bn-MeGlcA³Xyl₃

The catalytic activity of *Pes*GE was evaluated using Bn-MeGlcA^{3}Xyl$_3$ as a substrate. After *Pes*GE treatment, hydrolysis yielding benzyl alcohol was quantitatively monitored using HPLC (Fig. 4A and B). Additionally, hydrolyzed MeGlcA^{3}Xyl$_3$ was detected using TLC (Fig. S2). These results support using Bn-MeGlcA^{3}Xyl$_3$ as a substrate for GE activity assays. Importantly, the catalytic velocity of *Pes*GE for Bn-MeGlcA^{3}Xyl$_3$ was much higher than that for Bn-GlcA, which is widely used as a general substrate (Fig. 4C). This substrate preference prompted us to investigate the differences in kinetic parameters between Bn-MeGlcA^{3}Xyl$_3$ and Bn-GlcA in greater detail.

To further investigate the catalytic mechanism, the initial enzyme reaction rate versus substrate concentration was plotted with fitting using the Michaelis–Menten equation, as shown in Fig. 5. The kinetic parameters, K_m, V_{max}, and k_{cat} for Bn-MeGlcA^{3}Xyl$_3$ were 0.43 ± 0.01 mM, 55.5 ± 1.1 μmol min^{-1}·mg^{-1}, and 35.8 ± 0.7 s^{-1}, respectively. Therefore, the catalytic efficiencies (k_{cat}/K_m) of this enzyme for Bn-GlcA and Bn-MeGlcA^{3}Xyl$_3$ were 0.13 mM^{-1} s^{-1} and 83.8 mM^{-1} s^{-1}, respectively (Fig. 5A). By contrast, for Bn-GlcA, the V_{max} plateau was not
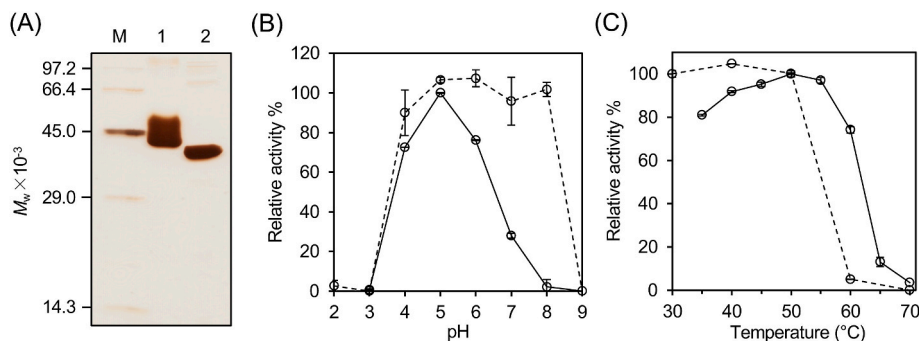

Fig. 3. Isolation and characterization of *Pes*GE. (A) SDS-PAGE of purified *Pes*GE: Lane M, standard protein molecular mass markers; lane 1, culture fluid; lane 2, deglycosylated *Pes*GE. Proteins were identified using silver staining. (B) Optimum pH (solid line) and pH stability (dotted line) for 6 h at 30 °C; (C) optimum temperature (solid line) and thermal stability (dot line) for 6 h at pH 5. Solid lines indicate the relative activity values under various pH and temperature conditions compared with ambient conditions (pH 5.0, 30 °C). Dotted lines indicate the residual activity values after exposure to various pH and temperature conditions for 6 h. Enzyme assays were conducted using 0.5 mM Bn-GlcA. The error bars indicate the standard deviation from three independent experiments.
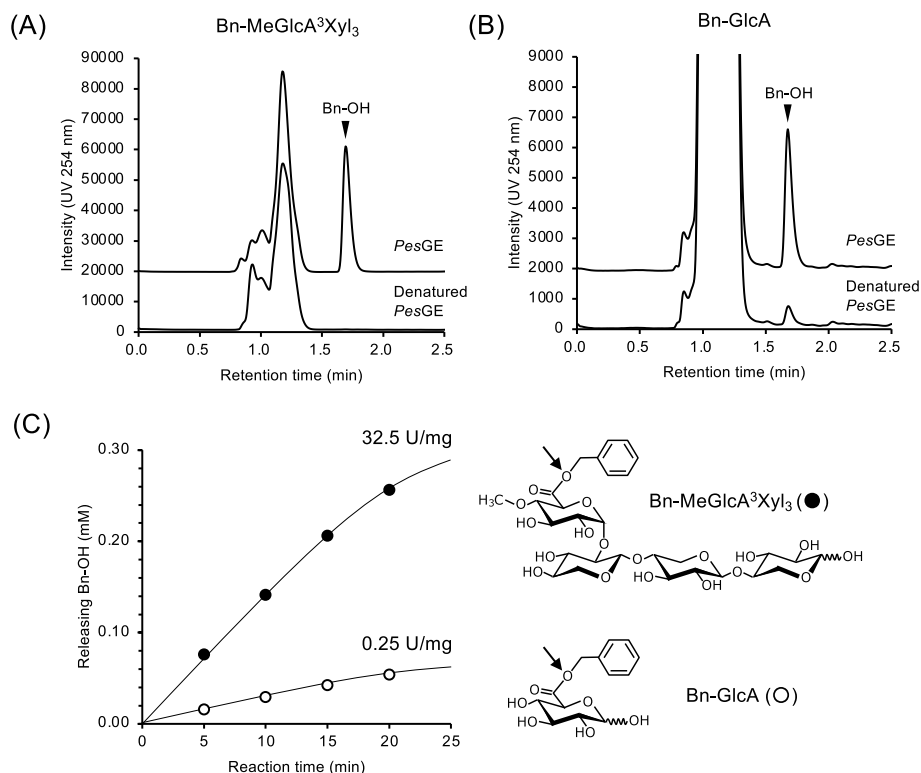
Fig. 4. Evaluation of *Pes*GE activity towards (A) Bn-MeGlcA³Xyl₃ and (B) Bn-GlcA. The upper row shows the hydrolysate after PesGE treatment (30 °C, pH 5.0, 20 min). The control reaction utilized the heat-denatured enzyme (boiling, 10 min), and its chromatogram is shown in the bottom row. The peak at 1.7 min corresponds to the benzyl alcohol (Bn-OH) standard retention time peak. (C) Comparison of the catalytic velocity of PesGE for Bn-MeGlcA³Xyl₃. (closed circles) and Bn-GlcA (open circles) as calculated using HPLC. One unit of enzyme activity was defined as the amount of enzyme that produces Bn-OH corresponding to 1 μmol.
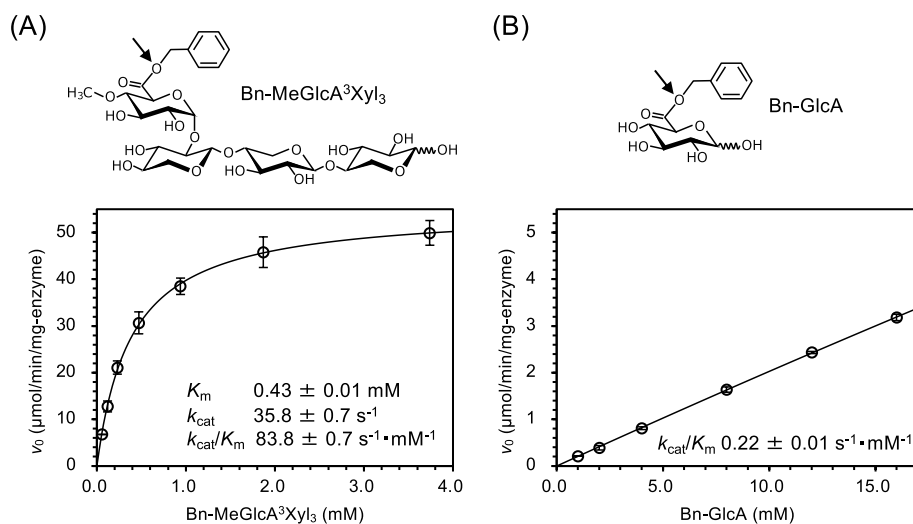

Fig. 5. Michaelis–Menten kinetic analysis of *Pes*GE toward (A) Bn-MeGlcA³Xyl₃ ([S]: 0.05–3.87 mM) and (B) Bn-GlcA ([S]: 0.01–16.0mM). Experimental data points are shown as circles. Best fits as obtained by non-linear least squares optimization of the Michaelis–Menten equation are shown as black lines. Error bars represent the standard deviation of three independent experiments.

observed at substrate concentrations of up to 16 mM. Thus, K_m and k_{cat} values could not be calculated (Fig. 5B). The extremely high K_m value for Bn-GlcA (K_m > 16 mM) indicated an extremely low binding affinity for Bn-GlcA. For Bn-MeGlcA³Xyl₃, the ester hydrolysis rate reached its maximum at substrate concentrations below 4 mM. The resulting k_{cat}/K_m value for Bn-MeGlcA³Xyl₃ was 645-fold higher than that for Bn-GlcA. These results suggest that the newly synthesized Bn-MeGlcA³Xyl₃ is an excellent substrate for kinetic analysis.

3.4. In silico docking analysis of PesGE with Bn-MeGlcA³Xyl₃

To elucidate the structural basis for the substrate preference of *Pes*GE, an *in silico* docking simulation was performed using MOE. Fig. 6 shows the modeling of Bn-MeGlcA³Xyl₃ and Bn-GlcA with the putative binding site of *Pes*GE. In both cases, key interactions were observed with five catalytic residues, Arg212, Lys215, Gln257, Glu265, and Trp308, associated with GlcA*p* hydroxyl group recognition [11]. Additional
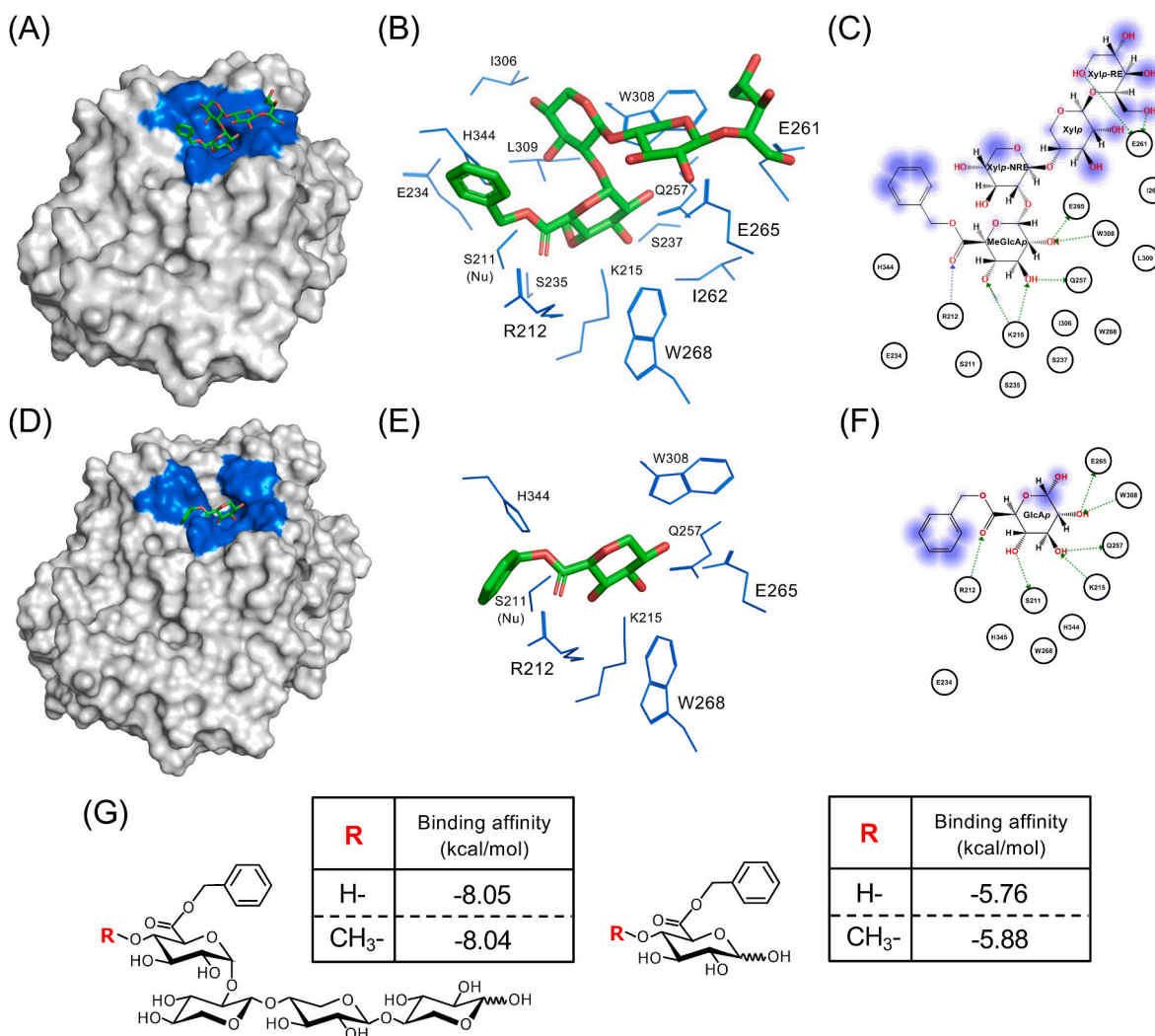
Fig. 6. Docking model for (A to C) Bn-MeGlcA³Xyl₃ and (D to F) Bn-GlcA binding to the active site pocket of *Pes*GE. (A and D) The blue-highlighted surface represents the region in contact with Bn-MeGlcA³Xyl₃ and Bn-GlcA. (B and E) Close-up views of the substrate-binding site. Binding site-related residues are shown as colored sticks. (C and F) 2D diagrams displaying residues in proximity around the ligand, indicating hydrogen-bonding interactions. The ligand is further annotated by a proximity contour and the magnitude of solvent exposure, while the residues are annotated by a reduction in solvent exposure. (G) The binding affinities of Bn-MeGlcA³Xyl₃, Bn-GlcA³Xyl₃, Bn-MeGlcA, and Bn-GlcA for *Pes*GE.

direct interactions between Glu261 and reducing-end Xyl*p* (Xyl*p*-RE) in Bn-MeGlcA³Xyl₃, involving two hydrogen bonds, were observed. These direct interactions suggested that the increased activity of Bn-MeGlcA³Xyl₃ in the observed kinetics could be due to the presence of the xylotriose moiety. Consequently, the binding affinities to Bn-MeGlcA³Xyl₃ and Bn-GlcA were −8.04 and −5.76 kcal mol⁻¹, respectively, indicating that the structure of Bn-MeGlcA³Xyl₃ is suitable for enzyme-substrate complex formation with *Pes*GE.

As described in previous reports, the 4-*O*-methyl group in GlcA*p* is a key structural determinant of GEs [11]. From this point of view, the highly conserved Leu309 residue is expected to come into contact with the 4-*O*-methoxy group of GlcA*p* via a hydrophobic interaction. Accordingly, the Leu309 residue was located near the methoxy group of GlcA*p*. To clarify the effects of the presence/absence of methylation at the 4-*O* position, 6-benzyl-4-*O*-methyl-D-glucuronate (Bn-MeGlcA), which had the methyl group at the 4-*O* position of MeGlcA*p*, was generated, and its binding energy was compared with that of Bn-GlcA based on the *in silico* simulation study (Fig. 6G). In the case of Bn-MeGlcA and Bn-GlcA, the binding affinities were calculated as −5.88 and −5.76 kcal mol⁻¹, respectively, indicating that the enhanced affinity due to the presence of 4-*O*-methylation at MeGlcA*p* is consistent

with that observed in the *in vitro* experiments [20]. In contrast, the binding affinities toward Bn-MeGlcA³Xyl₃ and 1,2³-α-D-(6-benzyl-D-glucuronyl)-1,4-β-D-xylotriose (Bn-GlcA³Xyl₃) lacking the 4-*O*-methylation did not significantly differ, with values of −8.05 and −8.04 kcal mol⁻¹, respectively. These unexpected results suggested that the stable substrate binding with Bn-MeGlcA³Xyl₃ could be predominantly owing to the presence of the xylan backbone rather than that of the 4-*O*-methyl group of GlcA*p*. In summary, the considerably enhanced binding affinity for Bn-MeGlcA³Xyl₃ may be attributed to the presence of the xylan backbone rather than the 4-*O*-methyl group of GlcA*p*, according to the kinetics and simulation study. In the future, the molecular mechanism underlying the substrate recognition of GE should be clarified based on this hypothesis using mutation analyses of *Pes*GE with Bn-MeGlcA³Xyl₃ and its derivatives.

4. Discussion

The natural polymeric substrate should be subjected to the individual enzymatic degradation systems from the viewpoints of gaining molecular basis to better understand the degradation mechanism and its utilization for lignocellulose biorefinery. In the case of GEs, the newly

synthesized Bn-MeGlcA^{3}Xyl$_3$ provides a good example. Structurally, Bn-MeGlcA^{3}Xyl$_3$ was expected to reflect the lignin and carbohydrate features of naturally occurring LCCs. Using Bn-MeGlcA^{3}Xyl$_3$, we successfully achieved the first productive kinetic parameters of GE. In other word, the feasibility of natural substrate synthesis was justified by the kinetic data obtained here.

The synthetic substrates, esterified GlcA or MeGlcA, have been used as core structure-containing forms. They are primarily divided into two substrate types that vary in aglycone or carbohydrate moieties. Two major structural characteristics are important for the substrate specificity of GE in response to GlcA moiety substitutions: i) the structural characteristics of the lignin-like benzyl alcohol portion of the ester [20] and ii) the presence of a 4-*O*-methyl substituent [20,22–24]. In the present study, we focused on the presence of a xylan backbone linked to the anomeric position of MeGlcA as the third characteristic for demonstrating considerable catalytic performance. The *in silico* docking simulation revealed the direct interaction between the xylotriose fragment attached to Bn-MeGlcA^{3}Xyl$_3$ and the Glu261 residue at the entry site of the catalytic pocket of *Pes*GE (Fig. 6C). This direct interaction has been observed in the crystallographic binding studies of both bacterial *Ot*GE15A and fungal *Cu*GE [11,25]. Particularly, these conserved Glu residues interacted with the hydroxy group of a Xyl*p*-RE residue at the reducing end of the xylotriose fragment. In contrast, no interaction was observed between Xyl*p*-NRE and Xyl*p* sequentially located next to MeGlcA*p* (Fig. 6C). These results suggested that at least three residues toward the reducing-end axis are required to capture a substrate molecule in the catalytic center of GEs. This finding indicated that GEs accessed the targeted ester through interactions with the xylan main chain. Notably, Bn-MeGlcA^{3}Xyl$_3$ is the first example that satisfies the three above-listed categories.

To gain in-depth insights into the considerable catalytic performance of Bn-MeGlcA^{3}Xyl$_3$, the impact of the presence of a 4-*O*-methyl substituent and the presence of a xylan backbone were compared in an *in silico* simulation (Fig. 6G). Notably, in the case of Bn-MeGlcA^{3}Xyl$_3$, the binding affinity of *Pes*GE was independent of the presence or absence of a 4-*O*-methyl substituent of GlcA*p*. This finding may be attributable to the fact that the two hydrogen bonds between the conserved Glu261 and hydroxy group of a Xyl*p*-RE residue were stronger than the hydrophobic interaction between the conserved Leu309 and 4-*O*-methyl group of MeGlcA*p* (Fig. 6G). Many researchers have overlooked this phenomenon because the synthetic substrates developed thus far lack the xylan main chain in their structure. It is well known that the modification of the 4-*O*-methyl group of MeGlcA*p* in xylan is not ubiquitous and varies depending on the plant species and tissues. For example, the xylan extracted from cotton seed possesses unmodified GlcA in its side chain [26]. In contrast, beechwood glucuronoxylan and oat-spelt arabinoglucuronoxylan contain methoxy substituents on MeGlcA [27]. To adapt to this plant species-dependent diversity in the 4-*O*-methyl modification of MeGlcA*p*, GE may act independently of the presence or absence of the 4-*O*-methyl group. In the near future, we aim to further develop and study a series of the natural core Bn-MeGlcA^{3}Xyl$_3$ for biochemical kinetic studies using these customized xylooligosaccharides derived from various plant species.

In conclusion, the newly synthesized natural core substrate Bn-MeGlcA^{3}Xyl$_3$ is useful for elucidating the catalytic mechanism and high-sensitivity screening of GEs isolated from environmental sources or mutant libraries. This achievement contributes substantially to the field by providing valuable insights into GE function and catalytic mechanisms. Furthermore, Bn-MeGlcA^{3}Xyl$_3$ demonstrates remarkable versatility in GE assays and serves as a platform substrate for investigating the enzymatic breakdown mechanisms of benzyl ester cross-linkages between lignin and glucuronoxylan. In the near future, various synthetic LCC derivatives will be developed using the natural core Bn-MeGlcA^{3}Xyl$_3$ as an initial template structure. These innovative synthetic approaches hold promise for advancing enzymatic degradation processes in industrial biomass refinery applications.

Data statement

All data generated or analyzed during this study are included in this published article.

CRediT authorship contribution statement

Sangho Koh: Writing – review & editing, Writing – original draft, Visualization, Validation, Methodology, Investigation, Formal analysis, Data curation, Conceptualization. **Yasuko Saito:** Writing – review & editing, Visualization, Validation, Formal analysis, Data curation. **Hisashi Kudo:** Writing – review & editing, Investigation. **Seiichi Taguchi:** Writing – review & editing. **Akio Kumagai:** Writing – review & editing. **Masahiro Mizuno:** Writing – review & editing, Supervision, Resources, Investigation, Funding acquisition, Data curation, Conceptualization. **Masahiro Samejima:** Writing – review & editing, Supervision, Conceptualization. **Yoshihiko Amano:** Writing – review & editing, Supervision, Project administration, Funding acquisition, Conceptualization.

Declaration of competing interest

The authors declare the following financial interests/personal relationships which may be considered as potential competing interests:

Sangho Koh reports financial support was provided by Japan Society for the Promotion of Science. Sangho Koh reports financial support was provided by Shinshu University Japan Society for the Promotion of Science. Masahiro Mizuno reports financial support was provided by Sugiyama Sangyou Kagaku Research Foundation. If there are other authors, they declare that they have no known competing financial interests or personal relationships that could have appeared to influence the work reported in this paper.

Appendix A. Supplementary data

Supplementary data to this article can be found online at https://doi.org/10.1016/j.bbrc.2024.150642.

References

[1] Y.M. Bar-On, R. Phillips, R. Milo, The biomass distribution on Earth, Proc. Natl. Acad. Sci. U. S. A 115 (2018) 6506–6511, https://doi.org/10.1073/pnas.1711842115.

[2] T. Watanabe, T. Koshijima, Evidence for an ester linkage between lignin and glucuronic acid in lignin–carbohydrate complexes by DDQ-oxidation, Agric. Biol. Chem. 52 (1988) 2953–2955, https://doi.org/10.1080/00021369.1988.10869116.

[3] P. Biely, Microbial glucuronoyl esterases: 10 years after discovery, Appl. Environ. Microbiol. 82 (2016) 7014–7018, https://doi.org/10.1128/AEM.02396-16.

[4] S. Spániková, P. Biely, Glucuronoyl esterase-novel carbohydrate esterase produced by *Schizophyllum commune*, FEBS Lett. 580 (2006) 4597–4601, https://doi.org/10.1016/j.febslet.2006.07.033.

[5] X.L. Li, S. Spániková, R.P. de Vries, P. Biely, Identification of genes encoding microbial glucuronoyl esterases, FEBS Lett. 581 (2007) 4029–4035, https://doi.org/10.1016/j.febslet.2007.07.041.

[6] H. Nishimura, A. Kamiya, T. Nagata, M. Katahira, T. Watanabe, Direct evidence for a ether linkage between lignin and carbohydrates in wood cell walls, Sci. Rep. 8 (2018) 6538, https://doi.org/10.1038/s41598-018-24328-9.

[7] S. Koh, M. Mizuno, Y. Izuoka, N. Fujino, N. Hamada-Sato, Y. Amano, Xylanase from marine filamentous fungus *Pestalotiopsis* sp. AN-7 was activated with diluted salt solution like brackish water, J. Appl. Glycosci. 68 (2021) 11–18, https://doi.org/10.5458/jag.jag.JAG-2020_0011.

[8] M. Mendonça, M. Barroca, T. Collins, Endo-1,4-β-xylanase-containing glycoside hydrolase families: characteristics, singylarities and similarities, Biotechnol. Adv. 65 (2023) 108148, https://doi.org/10.1016/j.biotechadv.2023.108148.

[9] O. Ryabova, M. Vršanská, S. Kaneko, W.H. van Zyl, P. Biely, A novel family of hemicellulolytic α-glucuronidase, FEBS Lett. 583 (2009) 1457–1462, https://doi.org/10.1016/j.febslet.2009.03.057.

[10] J. Jumper, R. Evans, A. Pritzel, T. Green, M. Figurnov, O. Ronneberger, K. Tunyasuvunakool, R. Bates, A. Žídek, A. Potapenko, A. Bridgland, C. Meyer, S.A. A. Kohl, A.J. Ballard, A. Cowie, B. Romera-Paredes, S. Nikolov, R. Jain, J. Adler, T. Back, S. Petersen, D. Reiman, E. Clancy, M. Zielinski, M. Steinegger, M. Pacholska, T. Berghammer, S. Bodenstein, D. Silver, O. Vinyals, A.W. Senior, K. Kavukcuoglu, P. Kohli, D. Hassabis, Highly accurate protein structure prediction with AlphaFold, Nature 596 (2021) 583–589, https://doi.org/10.1038/s41586-021-03819-2.

[11] H.A. Ernst, C. Mosbech, A.E. Langkilde, P. Westh, A.S. Meyer, J.W. Agger, S. Larsen, The structural basis of fungal glucuronoyl esterase activity on natural substrates, Nat. Commun. 11 (2020) 1026, https://doi.org/10.1038/s41467-020-14833-9.

[12] M. Wojciechowski, B. Lesyng, Generalized born model: analysis, refinement, and applications to proteins, J. Phys. Chem. B 108 (47) (2004) 18368–18376, https://doi.org/10.1021/jp046748b.

[13] C.R. Corbeil, C.I. Williams, P. Labute, Variability in docking success rates due to dataset preparation, J. Comput. Aided Mol. Des. 26 (6) (2012) 775–786, https://doi.org/10.1021/jp046748b.

[14] H.H. Huynh, M. Arioka, Functional expression and characterization of a glucuronoyl esterase from the fungus *Neurospora crassa*: identification of novel consensus sequences containing the catalytic triad, J. Gen. Appl. Microbiol. 62 (2016) 217–224, https://doi.org/10.2323/jgam.2016.03.004.

[15] S. Hüttner, S. Klaubauf, R.P. de Vries, L. Olsson, Characterisation of three fungal glucuronoyl esterases on glucuronic acid ester model compounds, Appl. Microbiol. Biotechnol. 101 (2017) 5301–5311, https://doi.org/10.1007/s00253-017-8266-9.

[16] M.D. Charavgi, M. Dimarogona, E. Topakas, P. Christakopoulos, E.D. Chrysina, The structure of a novel glucuronoyl esterase from *Myceliophthora thermophila* gives new insights into its role as a potential biocatalyst, Acta Crystallogr. D Biol. Crystallogr. 69 (2013) 63–73, https://doi.org/10.1107/S0907444912042400.

[17] C. Katsimpouras, A. Bénarouche, D. Navarro, M. Karpusas, M. Dimarogona, J. G. Berrin, P. Christakopoulos, E. Topakas, Enzymatic synthesis of model substrates recognized by glucuronoyl esterases from *Podospora anserina* and *Myceliophthora thermophila*, Appl. Microbiol. Biotechnol. 98 (2014) 5507–5516, https://doi.org/10.1007/s00253-014-5542-9.

[18] J.A. Arnling Bååth, N. Giummarella, S. Klaubauf, M. Lawoko, L. Olsson, A glucuronoyl esterase from *Acremonium alcalophilum* cleaves native lignin-carbohydrate ester bonds, FEBS Lett. 590 (2016) 2611–2618, https://doi.org/10.1002/1873-3468.12290.

[19] P.R. Pokkuluri, N.E.C. Duke, S.J. Wood, M.A. Cotta, X.L. Li, P. Biely, M. Schiffer, Structure of the catalytic domain of glucuronoyl esterase Cip2 from *Hypocrea jecorina*, Proteins 79 (2011) 2588–2592, https://doi.org/10.1002/prot.23088.

[20] C. d'Errico, J.O. Jørgensen, K.B.R.M. Krogh, N. Spodsberg, R. Madsen, R. N. Monrad, Enzymatic degradation of lignin-carbohydrate complexes (LCCs): model studies using a fungal glucuronoyl esterase from *Cerrena unicolor*, Biotechnol. Bioeng. 112 (2015) 914–922, https://doi.org/10.1002/bit.25508.

[21] D.W.S. Wong, V.J. Chan, A.A. McCormack, J. Hirsch, P. Biely, Functional cloning and expression of the *Schizophyllum commune* glucuronoyl esterase gene and characterization of the recombinant enzyme, Biotechnol. Res. Int. 2012 (2012) 951267, https://doi.org/10.1155/2012/951267.

[22] S. Spániková, M. Poláková, D. Joniak, J. Hirsch, P. Biely, Synthetic esters recognized by glucuronoyl esterase from *Schizophyllum commune*, Arch. Microbiol. 188 (2007) 185–189, https://doi.org/10.1007/s00203-007-0241-x.

[23] H.H. Huynh, N. Ishii, I. Matsuo, M. Arioka, A novel glucuronoyl esterase from *Aspergillus fumigatus*-the role of conserved Lys residue in the preference for 4-O-methyl glucuronoyl esters, Appl. Microbiol. Biotechnol. 102 (2018) 2191–2201, https://doi.org/10.1007/s00253-018-8739-5.

[24] M. Duranová, J. Hirsch, K. Kolenová, P. Biely, Fungal glucuronoyl esterases and substrate uronic acid recognition, Biosci. Biotechnol. Biochem. 73 (2009) 2483–2487, https://doi.org/10.1271/bbb.90486.

[25] S. Mazurkewich, J.N. Poulsen, L. Lo Leggio, J. Larsbrink, Structural and biochemical studies of the glucuronoyl esterase *Ot*CE15A illuminate its interaction with lignocellulosic components, J. Biol. Chem. 294 (2019) 19978–19987, https://doi.org/10.1074/jbc.RA119.011435.

[26] N. Matsuo, S. Yoshida, I. Kusakabe, K. Murakami, Chemical structure of xylan in cotton-seed cake, Aric Biol. Chem. 55 (1991) 2905–2907. https://doi.org/10.1271/bbb1961.55.2905.

[27] P. Biely, A. Malovíková, I. Uhliariková, X.L. Li, D.W.S. Wong, Glucuronoyl esterases are active on the polymeric substrate methyl esterified glucuronoxylan, FEBS Lett. 589 (2015) 2334–2339, https://doi.org/10.1016/j.febslet.2015.07.019.